



City Research Online

## City, University of London Institutional Repository

---

**Citation:** Bedi, S. S., Mallesha, V., Mahesh, V., Mahesh, V., Mukunda, S., Negi, S. & Ponnusami, S. A. (2023). Thermal characterization of 3D printable multifunctional graphene-reinforced polyethylene terephthalate glycol (PETG) composite filaments enabled for smart structural applications. *Polymer Engineering & Science*, doi: 10.1002/pen.26409

This is the published version of the paper.

This version of the publication may differ from the final published version.

---

**Permanent repository link:** <https://openaccess.city.ac.uk/id/eprint/30823/>

**Link to published version:** <https://doi.org/10.1002/pen.26409>

**Copyright:** City Research Online aims to make research outputs of City, University of London available to a wider audience. Copyright and Moral Rights remain with the author(s) and/or copyright holders. URLs from City Research Online may be freely distributed and linked to.

**Reuse:** Copies of full items can be used for personal research or study, educational, or not-for-profit purposes without prior permission or charge. Provided that the authors, title and full bibliographic details are credited, a hyperlink and/or URL is given for the original metadata page and the content is not changed in any way.

---


City Research Online:

<http://openaccess.city.ac.uk/>

[publications@city.ac.uk](mailto:publications@city.ac.uk)

---

# Thermal characterization of 3D printable multifunctional graphene-reinforced polyethylene terephthalate glycol (PETG) composite filaments enabled for smart structural applications

Surjeet Singh Bedi<sup>1</sup> | Vasu Mallesha<sup>1</sup>  | Vinyas Mahesh<sup>2,3</sup>  |  
Vishwas Mahesh<sup>4,5</sup>  | Sriram Mukunda<sup>6</sup> | Sushanth Negi<sup>2</sup> |  
Sathiskumar Anusuya Ponnusami<sup>3</sup>

<sup>1</sup>Department of Production Engineering, National Institute of Technology, Tiruchirappalli, India

<sup>2</sup>Department of Mechanical Engineering, National Institute of Technology, Silchar, India

<sup>3</sup>Department of Engineering, City, University of London, London, UK

<sup>4</sup>Department of Aerospace Engineering, Indian Institute of Science (IISc), Bangalore, India

<sup>5</sup>Department of Industrial Engineering and Management, Siddaganga Institute of Technology, Tumkur, India

<sup>6</sup>Department of Mechanical Engineering, Nitte Meenakshi Institute of Technology, Bangalore, India

## Correspondence

Vasu Mallesha, Department of Production Engineering, National Institute of Technology, Tiruchirappalli, India.  
Email: [vasu.m.manu@gmail.com](mailto:vasu.m.manu@gmail.com)

Vinyas Mahesh, Department of Mechanical Engineering, National Institute of Technology, Silchar, Assam 788010, India.  
Email: [vinyas.mahesh@gmail.com](mailto:vinyas.mahesh@gmail.com)

## Funding information

NITT/R&C/SEED GRANT, Grant/Award Number: /2021-22/PROJ.NO.49; Department of Science and Technology; Scheme for Young Scientists and Technologists, Grant/Award Number: SP/YO/2021/1652

## Abstract

The focus on fillers' influence in high-performance polymer composites has undergone a transformation. Additionally, the utilization of additive manufacturing (AM) in this venture has aroused the curiosity of investigators to empirically enumerate the characteristics of such composites for numerous applications. Consequently, this investigation aims to assess the thermal behavior of polyethylene terephthalate glycol (PETG) polymers reinforced with graphene flakes. As mentioned above, various weight ratios of the constituents are manufactured, blended, and extruded into six distinct varieties of 3D-printable filaments utilizing a twin-screw extruder. In accordance with the relevant American Society for Testing and Materials (ASTM) standards, we perform the thermal characterization of the compounded PETG/graphene pellets using Fourier transform-infrared (FTIR) spectroscopy, thermogravimetric analysis (TGA), and differential scanning calorimetry (DSC). The results reveal that enhancing the concentration of graphene augments the thermal properties of the composites. Furthermore, the FTIR investigation contributes to graphene's proficiency in absorbing infrared radiation and curbing micro-vibrations. Additionally, the study highlights the way in which chemical interactions between graphene and PETG impact the general effectiveness of the composites.

This is an open access article under the terms of the [Creative Commons Attribution](https://creativecommons.org/licenses/by/4.0/) License, which permits use, distribution and reproduction in any medium, provided the original work is properly cited.

© 2023 The Authors. *Polymer Engineering & Science* published by Wiley Periodicals LLC on behalf of Society of Plastics Engineers.

**KEYWORDS**

differential scanning calorimetry, differential thermogravimetric, fourier transform-infrared spectroscopy, graphene, polyethylene terephthalate glycol, thermogravimetric analysis

**Highlights**

- Thermal characterization of PETG/graphene composites used for AM is performed.
- FTIR, DSC, and TGA tests were carried out.
- Significant influence of graphene on thermal performance is witnessed.
- Useful for smart electro-mechanical devices.

## 1 | INTRODUCTION

With the development of rapid prototyping (RP) techniques, there has been an increase in inquisitiveness in finding appropriate polymers and their composites for particularly challenging applications such as medical, electronics, aerospace, and automotive due to the distinctive mechanical, thermal, and physical properties of polymers and polymer composites. Polymer composites have paved the way for extensive study in the field and offered innovative solutions to contemporary problems. The multifunctional properties of polymers, such as mechanical strength, biocompatibility, and environmental degradability, make them widely used. Examples include polyethylene terephthalate glycol (PETG), polylactic acid (PLA), acrylonitrile butadiene styrene (ABS), and others. These polymers' poor thermal performance, however, places a limit on their potential. To overcome this drawback, significant progress has been made in materials science recently in the creation of composite materials with improved qualities for various applications. There is much interest in the incorporation of filler materials like microparticles, fibers, carbon nanotubes (CNTs), and nanofillers into polymer matrices, which produce composites and nanocomposites. These nanocomposites are extremely desirable for various applications, as mentioned above, because of their outstanding mechanical, electrical, thermal, and barrier properties.<sup>1,2</sup>

Polymer nanocomposites have been created using carbon-based nanofillers like carbon nanofibers, CNT, and carbon black; among these, CNT has emerged as an exceptionally competent conductive filler. Nevertheless, the production expense associated with carbon nanotubes remains a primary obstruction. Considering this, researchers have sought to devise an economical substitute for carbon nanotubes, with the breakthrough discovery of graphene proving to be an auspicious development. The advent of graphene-based composites represents a new class of materials with enormous potential for a range of different uses. Graphene is a 2D material with exceptional

thermal, electrical, and mechanical properties. Its exceptional characteristics have led to a significant increase in research focused on its incorporation in polymer composites. Researchers have recently investigated the thermal properties of thermoplastic composites incorporated with graphene, particularly for 3D printing apps.<sup>2-4</sup> Graphene is anticipated to manifest extraordinary characteristics, encompassing elevated thermal conductivity, exceptional mechanical attributes, and outstanding electronic transport characteristics.<sup>5-8</sup> The distinctive characteristics of graphene have elicited significant intrigue for its prospective integration into a multitude of devices. In contrast to carbon nanotubes, which were a favorable filler option for composites prior to graphene's isolation, the superior surface-to-volume ratio of graphene stems from the unavailability of the molecules of polymer on interior nanotube surfaces. Consequently, this underscores the potential suitability of graphene for augmenting polymer composites' thermal and mechanical features. The addition of fillers like graphene has further improved the performance of these composites, making them suitable for advanced applications.<sup>9</sup> Stankovich et al.<sup>10</sup> looked into the potential uses of composite materials based on graphene. They focused on these composites' extraordinary mechanical strength and electrical conductivity as they detailed their creation, structure, and characteristics. The morphological properties, thermal, and mechanical characteristics of a thermoplastic elastomer made of polyethylene and recycled rubber were improved by the inclusion of graphene, according to Paran et al.<sup>11</sup> including its tensile strength and tensile modulus, crystallinity, and thermal stability. The addition of graphene oxide improved the nanocomposites' thermal stability and mechanical strength. The structural disparity of graphene-based materials can significantly impact the surface and thermo-mechanical properties of polymer composites. The impact of structural disparity of graphene-based materials on thermoplastic polyurethane (TPU) nanocomposites was studied by Bera and Maji.<sup>12</sup> Similarly, the impact of graphene oxide (GO) on the thermal and mechanical characteristics of

graphene oxide/hytrex (HTL) nanocomposites was investigated by Pandey et al.<sup>13</sup> The study reveals that GO inclusion brings about enhancements in both the mechanical and thermal characteristics of the material, including substantial enhancements in both the tensile strength and storage modulus. This leads the authors to suggest that GO/HTL nanocomposites hold great potential for application in structural engineering. Liu et al.<sup>14</sup> examined the thermal characteristics and mechanical characteristics of GO-reinforced epoxy resin nanocomposites. The study revealed that GO incorporation notably heightened the composites' flexural and tensile strength and their storage modulus. Moreover, the nanocomposites exhibited improved thermal stability and glass transition temperature. At a modest loading of 0.15 wt%, Liao et al.'s<sup>15</sup> investigation into adding graphene to polyurethane acrylates revealed intriguing improvements in the rheological, mechanical, electrical, and thermal characteristics of the resultant nanocomposites. This discovery highlights the positive potential of graphene as a nanofiller in polyurethane acrylate matrices. Examining the surface characteristics of thermoplastic polyurethane (TPU) composites reinforced with GO and reduced graphene oxide (RGO) is an intriguing area for investigation. There is currently little information on how the structural differences between GO and RGO influence their interaction with TPU. For enhanced comprehension of how the structure of graphene influences the characteristics of TPU nanocomposites, more research is necessary in this area. Similar to this, Wang et al.<sup>16</sup> examined how adding graphene to CF/PPBESK composites affected their mechanical and thermal conductivity qualities. The outcomes showed that the graphene-modified composites formed a conductive network, leading to appreciable increases in heat conductivity. Additionally, by passivating cracks and preventing crack development, graphene increased the mechanical characteristics of the composites. These increases in interlaminar shear strength (ILSS), compressive strength, and flexural strength (FS) demonstrate the promise of graphene-modified composites for structural applications. In contemporary research, a body of literature exists where the utilization of graphene nanoplatelets (GNPs) as fillers has been explored to augment the characteristics of the epoxy composite.<sup>17,18</sup> The emergence of hybrid composite materials, characterized by their multifaceted mechanical, thermal, and electrical attributes, has piqued the interest of scholars.<sup>19,20</sup>

Similarly, numerous researchers have conducted investigations to explore the impact of graphene and other fillers on metals, ceramics, and other thermoplastics, aiming to determine their potential applications across diverse fields. Graphene is employed to reinforce not only

polymer matrix materials but also metal and ceramic composites, leveraging its remarkable attributes.<sup>21–23</sup> A groundbreaking technique for producing GO-reinforced epoxy resin nanocomposites was introduced by Yang et al.<sup>24</sup> Through a two-phase extraction process, 0.0375 wt% GO incorporation led to remarkable compressive failure strength and toughness enhancement. Although the process was somewhat intricate, the study presents a promising approach to fabricating GO-epoxy resin nanocomposites. Overall, the authors inferred that GO functions as a potent reinforcing agent for epoxy resin nanocomposites. By changing the concentration of graphene in a PC-ABS matrix from 0.01 vol% to 0.25 vol%, Vijay et al.<sup>25</sup> examined the behavior of the material. The ensuing effects on microstructure, dimensional accuracy, and density were investigated. Additionally, the researchers probed the impact of heightened copper particle content on thermal conductivity in an ABS matrix. The incorporation of copper particles at 2.5 and 5 wt.% was examined, and the nanocomposites were compared for their thermal conductivity. The results disclosed that enhancing the concentration of copper causes the polymer nanocomposite's thermal conductivity to rise. To create fused filaments, Relinque et al.<sup>26</sup> concentrated on synthesizing and characterizing acrylonitrile-butadiene-styrene (ABS) composites with improved conductivity. The inclusion of conductive fillers enhanced the electrical conductivity of the composites. These outcomes demonstrate the potential of these composites for conductivity-required additive manufacturing applications. The potential of recycled PET as a sustainable substitute supply for 3D printing was looked at in the study by Patra and Negi.<sup>27</sup> The enhanced properties of the modified PET demonstrated its suitability as a replacement substance in ecologically friendly additive manufacturing techniques. In a study led by Mahesh et al.<sup>28</sup> the effects of incorporating organically modified montmorillonite (OMMT) nano clay and short carbon fibers (SCFs) into extruded PETG comonomers for use in 3D printing were investigated. The addition of SCFs and OMMT resulted in modifications of the chemical interactions within the comonomer blend, with more substantial alterations observed at higher weight percentages of these additives. Interestingly, the addition of OMMT reduced the comonomer blend's ability to absorb infrared light. However, at weight percentages above 3%, particle agglomeration was noted. Sahoo et al.<sup>29</sup> discovered that carboxylic acid functionalization enhances dispersion and boosts the mechanical performance of CNT composites. The study also highlights the influence of processing methods such as sonication and high-shear mixing on composite properties. Overall, the findings suggest that appropriate functionalization and processing can yield CNT composites with greater

thermal and mechanical characteristics. Billah et al.<sup>30</sup> examined the thermomechanical properties of short glass fiber-reinforced ABS and SCF for mass production with additive techniques. Results disclosed that the inclusion of fibers improved the composites' thermal stability, stiffness, and strength while increasing the viscosity and reducing the ductility. The findings have potential implications for the design and optimization of composite materials in large-scale additive manufacturing applications. Ramanathan et al.<sup>31</sup> demonstrated a remarkable rise in the glass transition temperature of poly(acrylonitrile) with only 1 wt.% of functionalized graphene sheets and a nearly 30°C improvement in poly (methyl methacrylate) with 0.05 wt.%. The mechanical properties showed a similar trend, with functionalized graphene sheet composites matching those of single-walled carbon nanotube-reinforced composites, underscoring the immense potential of functionalized graphene sheets in polymer composites.

In conclusion, the characteristics of the resultant composites have significantly improved as a result of the inclusion of graphene and its derivatives in polymer composites. These research demonstrate the enormous potential of graphene-based polymer composites in various applications like automobile, medical, and aerospace industries, etc., from improving mechanical and thermal properties to strengthening electrical conductivity and sustainability. More study in this area is necessary to explore the huge potential afforded by these new materials and their contribution to the development of numerous sectors. From the review, it was realized, to the best of authors' knowledge, that the works analyzing the thermal behavior of PETG/graphene composites is available in scarce. This work represents an initial endeavor in this aspect to understand the influence of graphene reinforcements on the thermal characteristics of PETG composites, which are the potential candidates for smart structures. The fabrication of five distinct PETG composites was undertaken, with varying concentrations of graphene, comprising 0.02, 0.04, 0.06, 0.08, and 0.1 wt.%. Thereafter, a comparative analysis of the thermal behavior of these composites was conducted using FTIR, DSC, and TGA, both among themselves and in relation to the neat PETG, to ascertain the thermal performance of the composite materials.

## 2 | MATERIALS AND METHODS

### 2.1 | Materials

The polymer material selected for the present experiment was PETG. It was procured from H R Organo Chem Pvt.

TABLE 1 Properties of graphene filler.

| Properties                                    | Values    |
|---|-----------|
| Thickness (nm)                                | 0.335     |
| Density (g/cm <sup>3</sup> )                  | 2.26      |
| Young's modulus (Gpa)                         | 1000      |
| Electrical conductivity (cm <sup>2</sup> /Vs) | 200,000   |
| Thermal conductivity (W/m.K)                  | 5000–5300 |
| Tensile strength (GPa)                        | 130       |

TABLE 2 Compositions of PETG composites.

| Specimens                    | PETG (wt.%) | Graphene (wt.%) |
|------------------------------|-------------|-----------------|
| PETG (A)                     | 100%        | 0%              |
| PETG+0.02 wt.% graphene (B1) | 99.98%      | 0.02%           |
| PETG+0.04 wt.% graphene (B2) | 99.96%      | 0.04%           |
| PETG+0.06 wt.% graphene (B3) | 99.94%      | 0.06%           |
| PETG+0.08 wt.% graphene (B4) | 99.92%      | 0.08%           |
| PETG+0.1 wt.% graphene (B5)  | 99.90%      | 0.1%            |

Ltd., Mumbai, India, along with the requisite graphene. According to the vendor's specification, the untreated PETG material possesses 49 MPa, 64 Mpa, and 1800 MPa of tensile strength, flexural modulus, and strength, respectively. As per the manufacturer's data, the molded components created using these pellets exhibited a yield strength of 49 MPa with a 4.5% elongation, accompanied by a bulk density of 1.28 g/cm<sup>3</sup>. Table 1 provides the properties of graphene, which is a hexagonally arranged single layer of carbon atoms.

Six distinct composite compositions were synthesized with varying concentrations of graphene, ranging from 0.02 to 0.1 weight percentage, as detailed in Table 2. The constituent components were blended using mechanical means to achieve the desired composition, and the resulting amalgamated pellets were fabricated through a twin-screw extrusion process.

### 2.2 | Extrusion of 3D printed filaments and material compounding

To create composite pellets, the mixes were subsequently combined utilizing a lab-scale twin-screw extruder (ZV-20). Table 3 provides a description of the extruder's specifications. With a consistent 4.5 N-m motor torque operating at 110 rpm and maintaining die temperatures within the range of 285–300°C, a steady pellet output of roughly 10 kg/h was attained. Table 4 lists the extruder's

observed zone temperatures during the compounding operation. The pellets were then extruded into thin monofilaments with a diameter of 1.75 mm after being pre-dried at around 60°C for 4 h. A filament-winding device was used during the extrusion process, and it was affixed to the final stage of the extrusion line. The extruded filaments were simultaneously coiled onto various spools throughout this procedure. It is crucial to note that creating smooth filaments after the addition of graphene to PETG presented certain difficulties. This was principally caused by the higher temperatures that were seen in the zone as a result of the inclusion of the graphene. The small piece of the filament of every composite was utilized to test the thermal characteristics of the composite, as shown in Figure 1.

### 2.3 | Fourier transform-infrared spectroscopy (FTIR)

The ASTM E-1252 standard was followed when conducting the FTIR investigations. High-grade spectroscopic grade potassium bromide (KBr), purchased from Sigma Aldrich and finely pulverized before being put onto the sample holder, was used to create the blank sample. The Perkin Elmer Spectrum 2 instrument's FTIR chamber then received this holder in order to do a background scan. The blank sample was taken out once the background scan was obtained. The compounded pellets were then crushed into a powder, and 5–8 milligrams of that powder were combined with spectroscopic-grade KBr. This mixture was relocated to a cylindrical block die

assembly after being further ground into powder in an agate mortar. For 2 min, a load of 10 tonnes was applied to generate a cylindrical disc specimen. The samples were then examined using the Perkin Elmer Spectrum 2 equipment (Figure 2A), which used IR light with a resolution of 4 cm<sup>-1</sup> and a wavelength range of 400 to 4000 cm<sup>-1</sup>. The specimens were generally 12 mm in size. To create a plot and obtain the complete spectrum, the percentage dissimilarity in the compounds' transmittance was plotted against the respective wavenumbers. In FTIR research, this methodology guarantees accurate and precise results.

### 2.4 | Thermo-gravimetric analysis (TGA)

Through TGA testing, the thermal behavior of the specimens was evaluated in accordance with ASTM E1131. The Perkin Elmer TGA 4000 analyzer (Figure 2B) was employed to analyze the specimens. The tests were carried out using a steady heating rate of 10°C/min at temperatures ranging from 32.10 to 750°C. To determine the net effective residue, the specimens were heated to 600°C in a nitrogen (N<sub>2</sub>) gas atmosphere at a constant flow rate of 20 mL/min, and subsequently oxygen (O<sub>2</sub>) gas was added at the same flow rate. To measure the deterioration temperature, onset temperature, and rate, the test was carried out. This made it possible to plot both the change in weight percentage to temperature (TG curve) and the weight change rate to temperature (DTG curve).

### 2.5 | Differential scanning calorimetry (DSC)

The DSC SETLINE analyzer (Figure 2C) was utilized to obtain thermograms for the composites through DSC following the guidelines set by ASTM D3418. The pellets of the samples were placed in the DSC chamber's sample container for assessment. The DSC measurements were conducted from ambient temperature to 400°C at a constant heating rate of 10°C/min and a steady supply of nitrogen gas at a rate of 50 mL/min. Phase transitions, exothermic and endothermic processes, major transition temperatures, and other critical elements of the composites were studied

TABLE 3 Twin-screw extrusion line specifications.

| Parameters                       | Values              |
|----------------------------------|---------------------|
| Screw L/D ratio                  | 40                  |
| Screw speed (rpm)                | 600                 |
| Screw diameter (mm)              | 21.5                |
| Production output (kg/h)         | Approx. 15 kg/h     |
| Melt pressure transducer (bar)   | 200                 |
| Maximum torque (N-m)             | 75 (for each shaft) |
| Melt temperature transducer (°C) | 400                 |

TABLE 4 Temperatures of the composites' compounding and filament extrusion.

| Temperatures for different processes (in °C) | Feed zone | Compression zone | Mixing zone | Die-head |
|--|-----------|------------------|-------------|----------|
| Compounding                                  | 275–285   | 280–295          | 290–300     | 285–305  |
| Extrusion                                    | 180–185   | 190–205          | 210–225     | 205–230  |

using thermograms created by graphing the change in heat energy against temperature.

## 2.6 | SEM characterization

The pellet form of the PETG composites was carefully inspected using a Hitachi S3500 SEM analyzer to

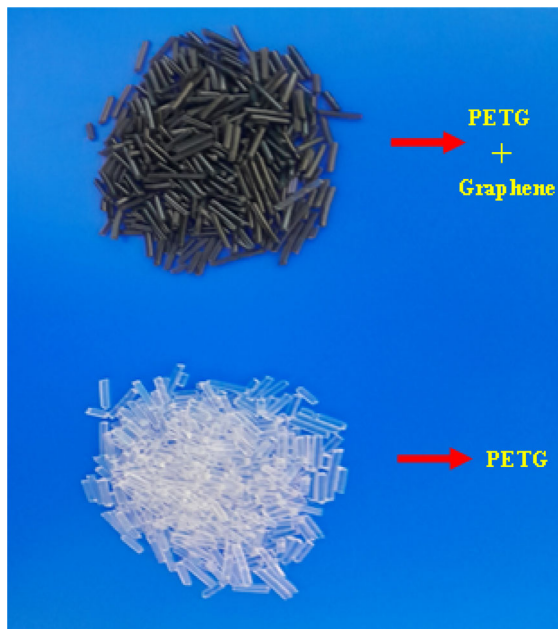


FIGURE 1 Specimens used for thermal testing.

determine the microstructure and dispersion of the graphene particles in the PETG composites. The low-energy secondary electron mode was used to accomplish this goal with a constant accelerating voltage of 10 kV. The print quality, bonding properties, and other potential causes of the fracture surfaces' failure were meticulously investigated.

## 3 | RESULTS AND DISCUSSION

Thermal stability is a crucial parameter in characterizing polymeric materials since the temperature often serves as a limiting factor in their application potential. The unique structure of graphene renders a substantial impact on the thermal characteristics of nanocomposites, warranting a thorough investigation thereof. In this regard, thermogravimetric analysis (TGA), Fourier transform-infrared (FTIR), and differential scanning calorimetry (DSC) were employed to assess the thermal stability of the virgin PETG and different variants of PETG/graphene polymer composites considered in this study.

### 3.1 | FTIR analysis

In view of this investigation, FTIR investigations are conducted to ascertain and analyze the chemical causes of failure. The clean PETG polymers' FTIR spectra are shown in Figure 3A. Due to the PETG molecule's

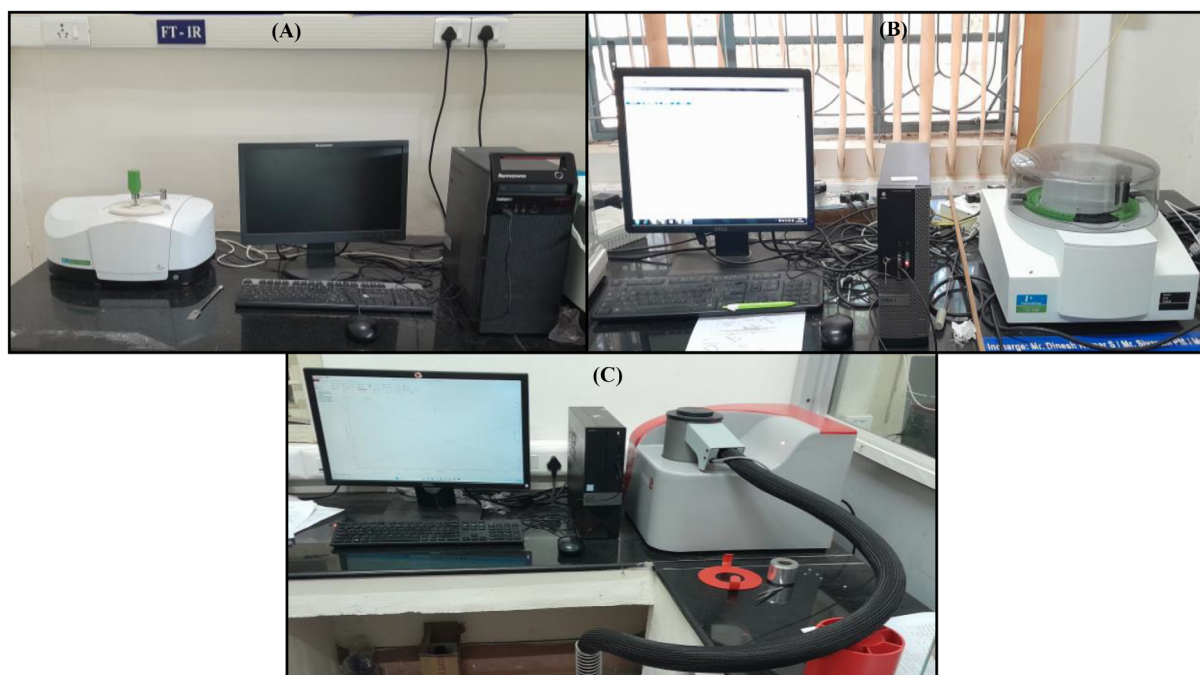


FIGURE 2 Experimental set-up of (A) FTIR instrument, (B) TGA analyzer, and (C) DSC analyzer.



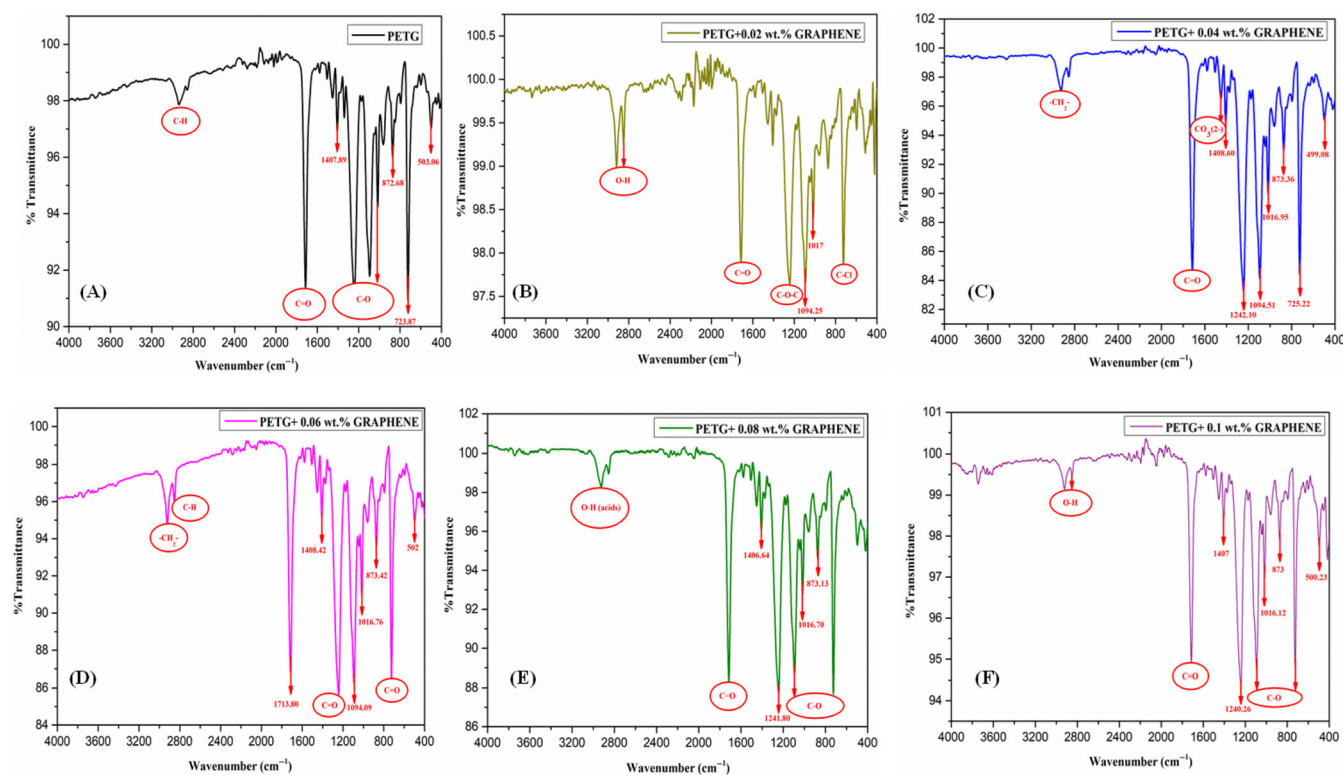


FIGURE 3 FTIR spectra of (A) PETG, (B) PETG +0.02 wt.% graphene, (C) PETG +0.04 wt.% graphene, (D) PETG +0.06 wt.% graphene, (E) PETG +0.08 wt.% graphene, and (F) PETG +0.1 wt.% graphene.

presence of C–H stretched alkanes, the molecules exhibit a slight drop in transmittance between 2850 and 2900  $\text{cm}^{-1}$ , as shown in the figure. These C–H groups absorb infrared radiation at this frequency range, resulting in a reduction in transmittance. This is a characteristic feature of PETG polymers. Strong prolongation of the ketone groups (C=O) occurs at 1710.23  $\text{cm}^{-1}$ . This is due to the presence of a relatively high concentration of ketone groups in the PETG polymer and due to the specific vibration and absorption characteristics of these functional groups. It suggests that the ketone functional groups are abundant and contribute significantly to the molecular structure and chemical properties of the PETG material. At 1407.89  $\text{cm}^{-1}$ , however, faint aromatic rotations are also seen. The deviation seen in the compound's fingerprint region at 1240.20  $\text{cm}^{-1}$ , 1093.38  $\text{cm}^{-1}$ , and 1016.67  $\text{cm}^{-1}$  is thought to be the result of bonds of ether in the molecule being bent and stretched by the C–O group. Near the far end of the fingerprint region, out-of-plane C–H bending vibrations of benzene derivatives are visible at 872.68  $\text{cm}^{-1}$  and 723.87  $\text{cm}^{-1}$ . The highest transmittance percentage is noticed at 503.06  $\text{cm}^{-1}$ , which affirms that 96.89% of heat is transmitted through the sample and the rest is absorbed. It is also noticed that the sample absorbs 8.5% more heat at the higher wavenumber than at the lower wavenumber.

The impact of graphene reinforcement on the molecular vibration of PETG composites is investigated and depicted in Figure 3B–F. Carboxylic or ketone groups can be found at 1712.14  $\text{cm}^{-1}$ , strong aromatic ethers can be found at 1241.26  $\text{cm}^{-1}$ , and aliphatic chloro compounds can be found at 723.84  $\text{cm}^{-1}$  in the fingerprint zone of composite with 0.02 wt.% of graphene. As can be seen from the FTIR spectrum in Figure 3B, when PETG is reinforced with graphene, the transmittance % increases compared to clean PETG, implying less IR spectrum absorption. Because of the O–H stretching vibrations present in the polymer composite sample, the molecules have a moderate increment in transmittance between 2850 and 2900  $\text{cm}^{-1}$  when compared to pure PETG.

Because there are more than 5 projections, it is a large molecular structure that can be seen in the composite with 0.04 wt.% of graphene, as shown in Figure 3C. Methylene group with some functional group bound to carbon is shown by the narrow projection at 2924.15  $\text{cm}^{-1}$ .

The cause of the drop in transmittance in PETG reinforced with 0.04 wt.% of graphene at 1713.90  $\text{cm}^{-1}$  is the significant stretching of the carboxylic group or ketonic group (C=O). The existence of methylene in the composite could also contribute to the drop in transmittance, as the carbonate ion at 1451.86  $\text{cm}^{-1}$  is a possibility.

Additionally, the high peaks in the fingerprint zone suggest that several functional groups, including phenol or tertiary alcoholic, aromatic ethers, alkyl substituted ethers, aliphatic phosphates, peroxides, aliphatic chloro compounds, and polysulfides, are being stretched out significantly. The plotted graph shows that increasing the weight percentage of graphene in PETG dampens the molecular vibrations in the polymer composite substantially.

The number of projections is likewise larger than 5, indicating a large molecular structure as seen in 0.06 wt.% of graphene reinforcement, as shown in Figure 3D. The existence of the methylene group may be detected by the projection at  $2921.81\text{ cm}^{-1}$ , and the reduction in transmittance can be absorbed because of the C–H extending of alkanes existing in the composite, as seen in pure PETG. When compared to pure PETG, the strong stretching of the ketonic group in the fingerprint zone can be detected at  $1241.96$  and  $724.99\text{ cm}^{-1}$ , resulting in a lower transmittance percentage and higher spectrum absorption.

The FTIR spectra of PETG reinforced with 0.08 weight percentage and 0.1 weight percentage, as shown in Figure 3E,F, of graphene in the polymer composite show an increment in the transmittance at  $2923.02\text{ cm}^{-1}$ , which is about 98%. This enhancement in the transmittance is more when compared to other composites of PETG with graphene. This can be credited to the existence of the O–H (acids) group at  $2923.02\text{ cm}^{-1}$ . The O–H stretching vibrations present in the polymer composite sample lead to a modest increase in transmittance between  $2850$  and  $2923.02\text{ cm}^{-1}$  when compared to pure PETG. But there is a large difference in the transmittance percentage at  $1713.93\text{ cm}^{-1}$  in 0.08 wt.% spectra and  $1717.42\text{ cm}^{-1}$  in 0.1 wt.% spectra. In 0.08 wt.% spectra, the transmittance percentage is 88.36, and 95.11 in 0.1 wt.% spectra. This difference is due to the less stretching of the ketonic group in 0.08 wt.% spectra as compared to 0.1 wt.% spectra. We can also observe this difference in the fingerprint zone. Functional groups present in the fingerprint zone are the same as other concentrations of graphene.

### 3.2 | Thermogravimetric (TGA) analysis

Through TGA research, the thermal stability characteristics of PETG composites have been examined, providing critical insights into their behavior. The TGA test was conducted using nitrogen and a range of temperatures between  $32.10^\circ\text{C}$  and  $750^\circ\text{C}$  at a heat rate of  $10^\circ\text{C}/\text{min}$ . In the study, crucial parameters like the start of degradation and the temperature of degradation have been

investigated. The results are included in this section along with a few key parameters, including the temperature at which degradation first starts to occur ( $T_i$ ) at 1% mass loss, the temperature at which it begins to occur at 10% mass loss ( $T_{10}$ ), the temperature at which it occurs at 50% mass loss ( $T_{50}$ ), the maximum temperature at which degradation has been observed ( $T_{\text{max}}$ ), and the amount of residue that remains after  $750^\circ\text{C}$ .

Figure 4 shows the thermogravimetric and differential thermogravimetric curves of clean polyethylene terephthalate glycol and its composites reinforced with graphene, which demonstrate the material's degradative activity. The findings show that PETG degrades at a temperature of about  $373.05^\circ\text{C}$  and that  $453.04^\circ\text{C}$  is the temperature at which degrading occurs at its fastest rate, as shown in Figure 4A. The PETG residual analysis shows very small amounts of residue, mostly made up of carbon, hydrogen, and oxygen atoms. Overall, these findings offer important new understandings of the factors influencing the thermal behavior of composites, which can be exploited to enhance their performance and attributes. Mahesh et al.'s<sup>28</sup> documentation of the TGA analysis for PETG has a similar justification.

The TGA and DTG curves shown in Figure 4B affirm that the thermal stability of the PETG +0.02 wt.% composite material is noticeably improved, as opposed to pure PETG. In specific, the initial degradation temperature at 1% mass loss ( $T_i$ ) increased from  $373.05^\circ\text{C}$  to  $385.24^\circ\text{C}$ , the degradation temperature at 10% weight loss ( $T_{10}$ ) increased to  $398.20^\circ\text{C}$ , the degradation temperature at 50% mass loss ( $T_{50}$ ) increased to  $424.25^\circ\text{C}$ , the maximum observed degradation temperature ( $T_{\text{max}}$ ) had an increase of  $473.04^\circ\text{C}$ , and the final leftover residue ( $m_f$ ) after  $750^\circ\text{C}$  is more as compared to neat PETG.

This enhancement in the thermal stability and residue percentage increase can be credited to the interfacial interaction between the graphene filler and PETG, illustrated in Figure 5.

The addition of graphene to a polymer nanocomposite (PNC) increased the degradation temperatures, according to earlier studies by Achaby et al.<sup>32</sup> This improvement in thermal stability is most likely the result of the volatile breakdown products' impeded diffusion inside the nanocomposites, which is strongly dependent. It has been discovered that graphene disperses reasonably well in PETG composite, which is probably because the two materials contact strongly at the interface due to the interactions between nanoparticles and polymer chains.

Incorporating 0.04 wt.% graphene to PETG composites is found to be a reliable strategy for enhancing their thermal stability, as illustrated in Figure 4C. The reinforcement of graphene at increasing weight percentages led to an increase in the composite's thermal stability.

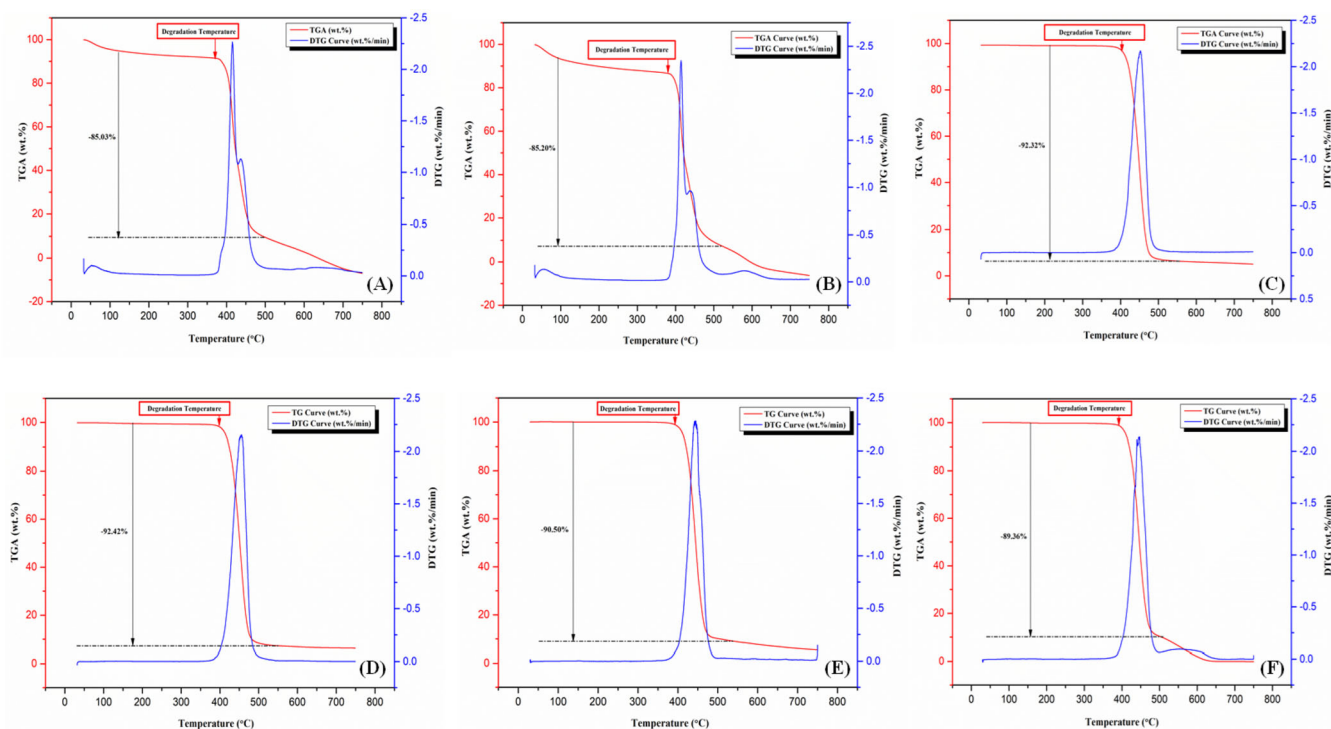


**FIGURE 4** Differential thermogravimetric (DTG) and thermogravimetric (TG) curves of (A) PETG, (B) PETG + 0.02 wt.% graphene, (C) PETG + 0.04 wt.% graphene, (D) PETG + 0.06 wt.% graphene, (E) PETG + 0.08 wt.% graphene, and (F) PETG + 0.1 wt.% graphene.

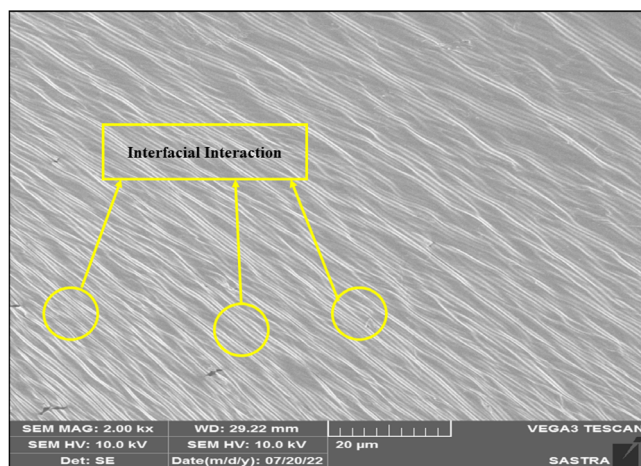


**FIGURE 5** SEM images of PETG + 0.02 wt.% graphene.

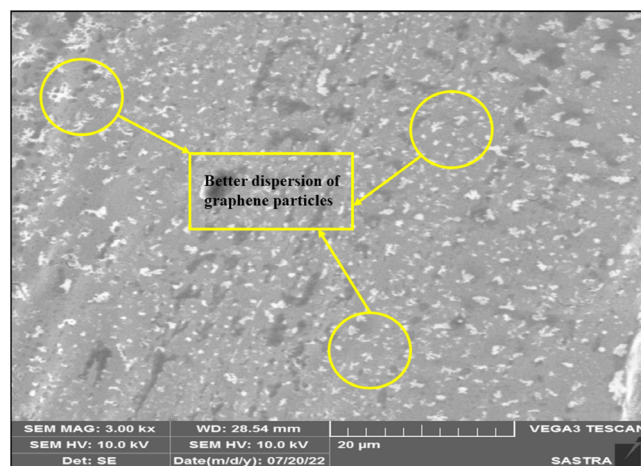


**FIGURE 6** SEM images of PETG + 0.04 wt.% graphene.

Remarkably, the final residue of the polymer composite increased as the amount of graphene added to the PETG + 0.04 wt.% graphene composite increased. In contrast, pure PETG displayed negligible final residue at 750°C. However, at the same temperature, incorporating graphene at concentrations ranging from 0.02 wt.% to 0.04 wt.% enhanced the final residue. Additionally, this composition showed an increment in  $T_i$ ,  $T_{10}$ ,  $T_{50}$ , and  $T_{max}$  by 29.67°C, 34.22°C, 26.51°C, and 29.02°C,

respectively, as compared to neat PETG. Similarly, these values also exceed in comparison to PETG + 0.02 wt.% graphene by 17.479°C, 23.89°C, 25.66°C, and 29.02°C, respectively.

The excellent dispersion of the graphene filler can be observed in Figure 6. This might be because PETG can be easily melted and processed. Strong shear forces are applied to the polymer during the melt mixing procedure, which helps to break up graphene agglomerates and

disperse the graphene particles evenly throughout the matrix. The addition of 0.04 wt.% graphene to PETG composites can enhance the material's heat dissipation capacity, leading to enhanced resistance to thermal degradation and thermal stability. Figure 4D presents the thermal gravimetric analysis (TGA) and derivative thermogravimetry (DTG) data of PETG +0.06 wt.% of graphene. The graph shows a notable improvement in

the composite's thermal stability compared to pure PETG and PETG +0.02 wt.% of graphene. However, it is slightly lower than the thermal stability of PETG reinforced with 0.04 wt.% graphene. The degradation process of the composite initiated at 401.41°C with 92.42% weight loss, followed by decomposition at 479.62°C. The enhancement in thermal stability was about 28.36°C when compared to the pure PETG, which can be credited to the good interfacial bonding between the PETG and graphene-reinforced PETG composites. Moreover, the homogeneously dispersed graphene acts as an outstanding insulator and a physical blockade for transporting volatile products during breakdown.

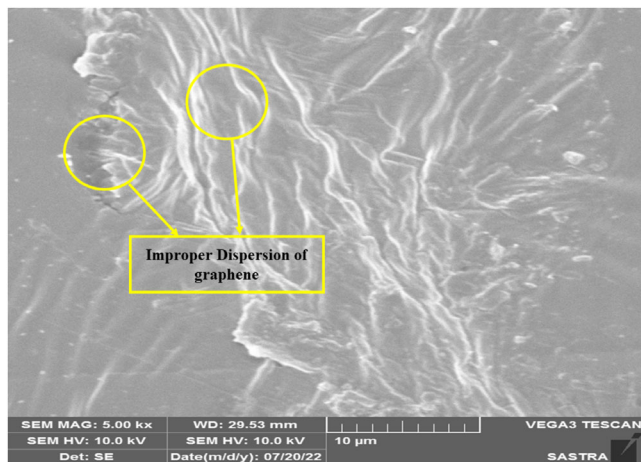


FIGURE 7 SEM images of PETG +0.08 wt.% graphene.

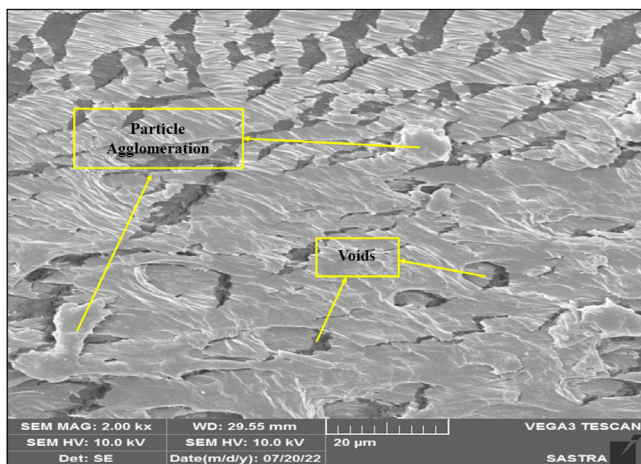


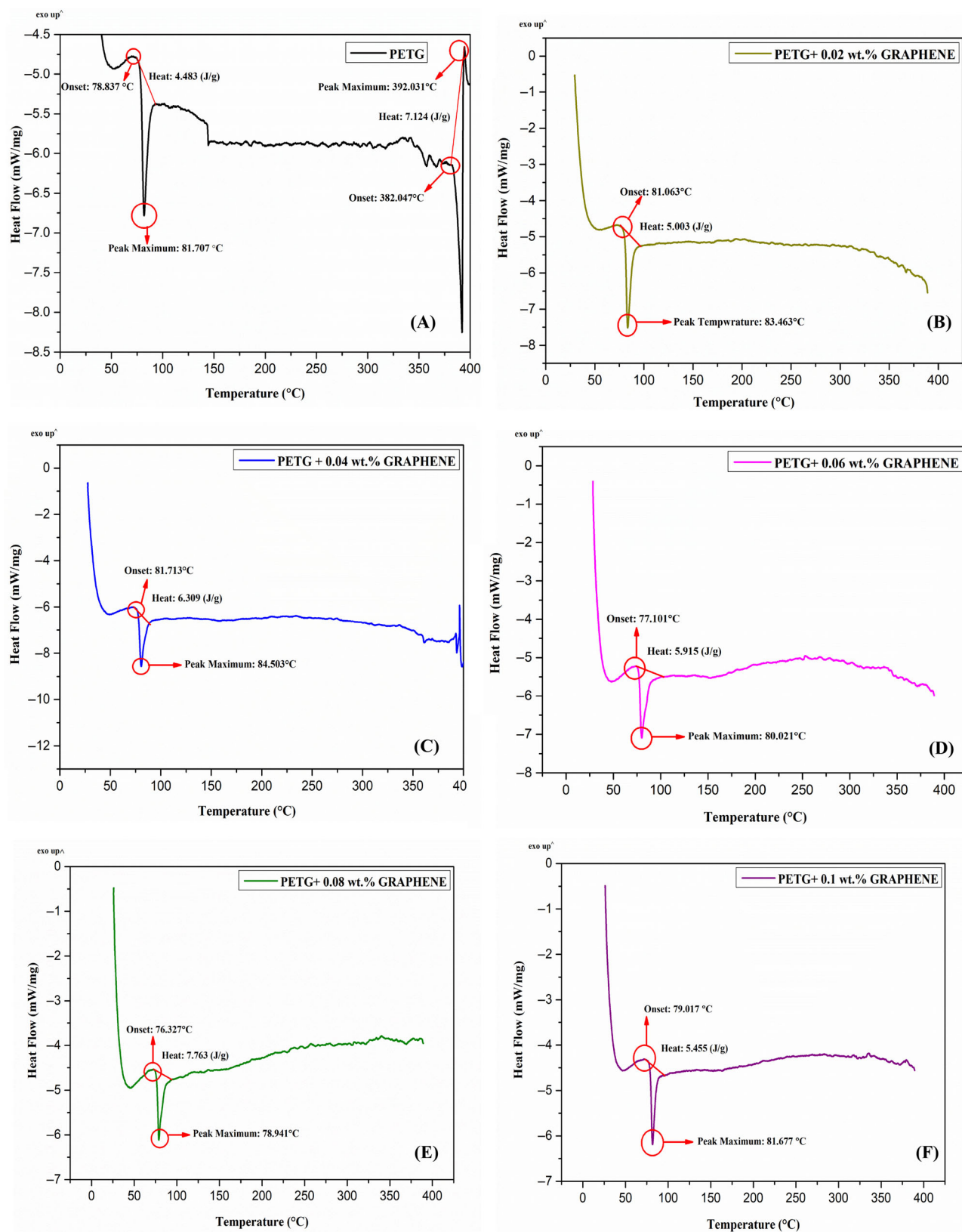
FIGURE 8 SEM images of PETG +0.1 wt.% of graphene.

Figure 4E presents the TGA and DTG curves of PETG +0.08 wt.% graphene filler. Notably, a discernible shift in the degradation temperature is apparent. Specifically, the onset degradation temperature was 394.64°C, slightly lower than the PETG +0.04 wt.% and PETG +0.06 wt.% of graphene. However, the composite with 0.08 wt.% of graphene still exhibited the ability to retain 50% of its initial weight at 445.40°C, indicating comparable thermal stability to the composite with 0.04 wt.% of graphene. These findings suggest that the 0.08 wt.% of graphene reinforcement did not reach the percolation threshold for PETG/graphene composites, thus differentiating its thermal properties from those of PETG composites with 0.02, 0.04, and 0.06 wt.% graphene fillers. This can also be credited to the improper dispersion of graphene in the PETG composite, as seen in Figure 7.

The thermal behavior of PETG +0.1 wt.% graphene composite is shown in Figure 4F. It can be revealed that incorporating 0.1 wt.% graphene to the PETG matrix increases the composites' thermal stability. The beginning deterioration is observed to start at 387.68°C with 50% of the starting weight still present at 446.53°C with the inclusion of 0.1 wt.% of graphene. However, the improvement in thermal stability was only slightly greater than that of the composites containing 0.02 wt.% and 0.08 wt.% of graphene in PETG composites. This could be explained by the existence of spaces and nanoparticle aggregation, which avoid the reliable

| Specimens | $T_i$ (°C) | $T_{10}$ (°C) | $T_{50}$ (°C) | $T_{max}$ (°C) | Residue (wt.%) at (750°C) |
|-----------|------------|---------------|---------------|----------------|---------------------------|
| PETG (A)  | 373.05     | 387.87        | 423.40        | 453.04         | 1.26                      |
| B1        | 385.241    | 398.20        | 424.25        | 473.04         | 2.34                      |
| B2        | 402.72     | 422.09        | 449.91        | 482.06         | 4.16                      |
| B3        | 401.41     | 419.64        | 447.72        | 479.62         | 3.03                      |
| B4        | 394.64     | 418.70        | 445.40        | 473.04         | 1.87                      |
| B5        | 387.68     | 418.68        | 446.53        | 475.29         | 2.45                      |

TABLE 5 DTG and TGA results of PETG and graphene-reinforced PETG composites.



**FIGURE 9** DSC (differential scanning calorimetry) thermogram of (A) PETG, (B) PETG + 0.02 wt.% graphene, (C) PETG + 0.04 wt.% graphene, (D) PETG + 0.06 wt.% graphene, (E) PETG + 0.08 wt.% graphene, and (F) PETG + 0.1 wt.% graphene.

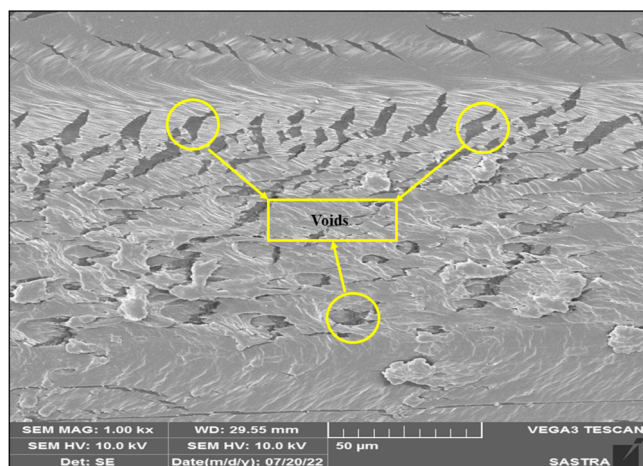


FIGURE 10 SEM images of polyethylene terephthalate glycol (PETG) reinforced with 0.06 wt.% of graphene.

TABLE 6 Glass transition temperature ( $T_g$ ) values of PETG and its composites.

| Specimens | Glass transition temperature ( $T_g$ ) ( $^{\circ}$ C) |
|-----------|--|
| PETG (A)  | 81.70  |
| B1        | 83.46  |
| B2        | 84.50  |
| B3        | 80.02  |
| B4        | 78.94  |
| B5        | 81.67  |

accretion of graphene elements on the surface. The agglomeration can result in intercalated microparticles and bigger aggregates, as seen in Figure 8, which eventually lower the heat resistance of the composites. The thermogravimetric analysis (TGA) results for the composites' major thermal properties are summarized in Table 5. The information includes vital temperature readings and residue values that are necessary for a thorough evaluation of the thermal properties of the composites. The goal of this presentation is to make the thermal behavior of each composite easier to understand and compare.

### 3.3 | Differential scanning calorimetry (DSC) analysis

The enthalpy fluctuations and critical phase transition temperature of PETG matrices within a specified range of temperature, spanning from ambient temperature to  $400^{\circ}$ C, were meticulously gauged employing DSC. To inspect the influence of various material additions on

the thermal efficiency of the composites, the experiments were conducted solely during the initial heating cycle.

By analyzing a DSC thermogram, which delineates the disparity in enthalpy as a function of temperature, the phase transitions were illustrated. The thermogram presented in Figure 9A manifests the DSC analysis of unmodified PETG polymers, from which it can be deduced that the glass transition temperature ( $T_g$ ) of neat PETG is  $81.70^{\circ}$ C. As the sample progressively assimilates heat energy, the curve exhibited by the material demonstrates a sustained descent, indicative of the material's thermal stability. At elevated temperatures approaching  $382.04^{\circ}$ C, the PETG sample begins to deteriorate and liquefy, as indicated by a substantial uptake of thermal energy.

The DSC thermogram of a PETG composite incorporated with a different weight percentage of graphene particles is shown in Figure 9B–F. The thermogram of composite PETG +0.02 wt.% of graphene shows a considerable change from a glassy state to a rubbery one around  $83.46^{\circ}$ C, commonly called the glass transition temperature ( $T_g$ ). This can be attributed to the graphene concentration, dispersion quality, and interfacial bonding between the graphene and the PETG. The required energy to raise the sample's temperature to the peak value is represented by the enthalpy associated with the peak temperature, which measures 5.003 J/g. In comparison to pure PETG, the  $T_g$  of the PETG composite has improved due to the inclusion of graphene particles, reaching  $83.46^{\circ}$ C, demonstrating that the material is now more thermally stable. The elimination of voids within the material brought on by the reinforcement of graphene is also responsible for the composite's continuous exothermic graph, which is free of any phase transitions. As seen in Figure 8, fewer voids encourage effective heat dissipation inside the composite, preventing any phase transition. The DSC thermogram for composite PETG +0.04 wt.% of graphene demonstrates that the glass transition temperature is improved, rising to  $84.50^{\circ}$ C. Moreover, the PETG +0.04 wt.% of graphene displays greater thermal stability than both the PETG and PETG +0.02 wt.% of graphene, as evidenced by the slight increase in the glass transition temperature. This enhancement can be attributed to the improved transfer of thermal loads between the graphene particle and the matrix, resulting in an extensive exothermic reaction above  $400^{\circ}$ C before melting. The alteration in the chemistry of the material observed in the spectra of FTIR is consistent with the findings in the differential scanning calorimetry thermogram of the composite, indicating that the composite's thermal resistance has improved. Furthermore, owing to the nucleation-inducing influence of

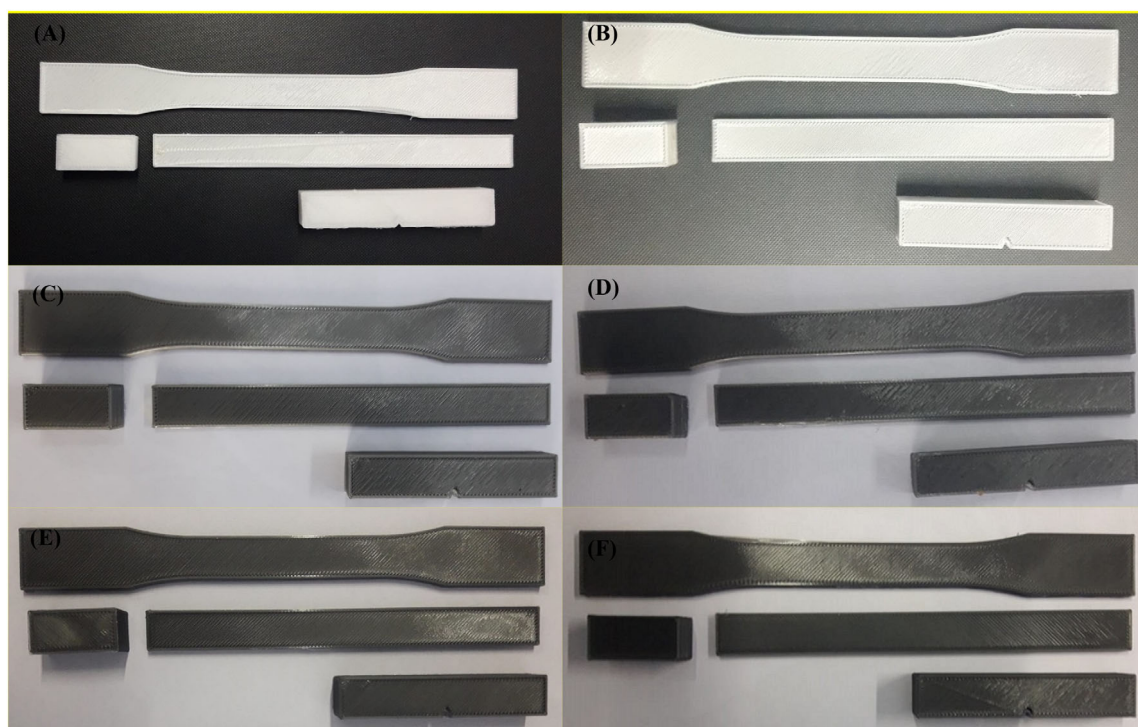


**FIGURE 11** 3D printed samples (A) PETG, (B) PETG +0.02 wt.% graphene, (C) PETG +0.04 wt.% graphene, (D) PETG +0.06 wt.% graphene, (E) PETG +0.08 wt.% graphene, and (F) PETG +0.1 wt.% graphene.

**TABLE 7** FDM 3D printing parameters for PETG and its composites.

| Parameters              | PETG        | PETG+ 0.02 wt.% graphene | PETG+ 0.04 wt.% graphene | PETG+ 0.06 wt.% graphene | PETG+ 0.08 wt.% graphene | PETG+ 0.1 wt.% graphene |
|-------------------------|-------------|--------------------------|--------------------------|--------------------------|--------------------------|-------------------------|
| Layer thickness         | 0.2         | 0.2                      | 0.2                      | 0.2                      | 0.2                      | 0.2                     |
| Raster angle (°)        | 45          | 45                       | 45                       | 45                       | 45                       | 45                      |
| Infill percentage (%)   | 100         | 100                      | 100                      | 100                      | 100                      | 100                     |
| Bed temperature (°C)    | 60          | 65                       | 70                       | 70                       | 75                       | 75                      |
| Infill shape            | Rectilinear | Rectilinear              | Rectilinear              | Rectilinear              | Rectilinear              | Rectilinear             |
| Printing speed (mm/s)   | 45          | 45                       | 45                       | 45                       | 45                       | 45                      |
| Nozzle temperature (°C) | 225         | 230                      | 235                      | 235                      | 240                      | 240                     |

graphene on the matrix, there is an augmentation in the crystalline structure of PETG composite, resulting in an elevation of the melting point towards higher temperatures. Incorporating a minute quantity of 0.06 wt.% graphene to PETG elicited a substantial decline in its glass transition temperature, which manifested as a discernible reduction to 80.02°C. This phenomenon can be attributed to the voids present within the matrix, as seen in Figure 10. The voids could have resulted from inadequate dispersion of the graphene particles within the matrix, leading to localized areas of reduced density and increased free volume. This, in turn, can cause a decrease in the T<sub>g</sub> of the composite material. Additionally, the disruption of hydrogen bonds that had developed between the graphene

and PETG composites due to the incorporation of a small amount of graphene particles could have contributed to the T<sub>g</sub> decline. Notably, no overt phase transition was evident in the composite material, as indicated by the continuous exothermic heat exchange observed above 400°C. The degradation of the composite material was detected to commence at a temperature of 370°C. In a similar fashion to the PETG +0.06 wt.% graphene composite, a decrease in the glass transition is obvious for the composite with 0.08 wt.% graphene. The observed glass transition temperature is 78.94°C, as depicted in the DSC graph, which illustrates the composite transition through an endothermic peak. The reduction in the glass transition is attributed to the emergence of aggregates, which serve as

defects, resulting in a decline in the melting temperature. As the graphene concentration rises, the likelihood of agglomeration formation also elevates, hindering the formation of molecular chains that constitute crystal lattices and reducing the degree of crystallinity. The PETG +0.1 wt.% graphene demonstrates the first peak at 81.67°C, indicating the  $T_g$  of the matrix. This temperature is found to be nearly identical to that of the pure PETG material. This similarity can be credited to the possibility of filler content clustering, resulting in a decrement in the composite's glass transition temperature. This phenomenon is consistent with previous studies. Table 6 represents the glass transition temperature values of PETG and its composites with graphene.

### 3.4 | Printability of the PETG and its composites

Polyethylene Terephthalate Glycol, or PETG, is a well-liked 3D printing filament recognized for its superior printability. Its printability is influenced by a number of factors, including strong layer adhesion, little shrinking, and little warping. A variety of 3D printers can use PETG since it is reasonably simple to extrude and has a wide printing temperature range. The resulting PETG graphene composites can display improved thermal qualities when PETG is mixed with graphene, as we discussed in the above sections.

Furthermore, the strong heat conductivity of graphene can also help lower the possibility of thermal deformation during the 3D printing process. PETG graphene composites might be more resistant to warping or distortion brought on by heat, which would enhance the dimensional stability and precision of printed products. Overall, the thermal properties of the composite material, including increased thermal conductivity, heat dissipation, and resistance to thermal deformation, can be improved by adding graphene to PETG. These characteristics make PETG graphene composites appropriate for uses needing effective thermal control and heat transfer. These properties also help while printing the PETG and PETG/graphene composites. The specimens printed from PETG and PETG/graphene composites are shown in Figure 11, and the necessary parameters are reported in Table 7.

## 4 | CONCLUSIONS

In this article, the characterization of the thermal properties of graphene-reinforced PETG composites used for fused deposition modeling is carried out. Six distinct

variations of PETG + graphene composites were considered for the investigation. The thermal characteristics of these composites were assessed by utilizing DSC, FTIR, and TGA methodologies. From the FTIR analyses, it was witnessed that adding graphene particles to PETG composites did not affect the chemical composition of the composites. Instead, the PETG molecules' ability to absorb IR light was decreased. Among all the compositions, the PETG +0.04 wt.% graphene demonstrated the most significant reduction in absorbance. However, when the weight percentage of graphene was raised to 0.1 wt.%, particle agglomeration was observed, and absorbance reduction was no longer evident.

On the other hand, the TGA investigations carried out on composites revealed a notable improvement in their thermal stability, particularly when exposed to temperatures exceeding 400°C. This enhancement is credited to the graphene reinforcements, which act as an effective thermal barrier, guarding the polymer against volatile compounds that may be expelled at higher temperatures. According to the TGA results, the thermal stability of the resultant composite is enhanced when graphene concentration in PETG composites increases, causing an increase in the onset degradation temperature. Out of all the different compositions examined, PETG infused with 0.04 weight percent of graphene exhibited the highest thermal stability, with the most significant upsurge in the onset degradation temperature. Finally, the DSC analyses revealed that the incorporation of 0.02 wt.% and 0.04 wt.% graphene particles exhibited a significant impact on the glass transition temperature ( $T_g$ ) of the composites. However, for other compositions, such as 0.06 weight percentage, 0.08 weight percentage, and 0.1 weight percentage, the  $T_g$  decreased, which can be credited to the deteriorated chemical interactions between the PETG and graphene particles, as well as the clustering of filler content. The constant exothermic heat exchange that was caused by the breakdown of hydrogen bonds at high temperatures followed the decrease in  $T_g$ . The PETG composites did not experience any substantial changes in the phase of the materials in the lack of such a response. Interestingly, DSC testing also demonstrated that PETG composites reinforced with 0.04 wt.% graphene exhibited the most favorable outcomes, highlighting the optimal concentration of graphene particles to achieve the desired improvements in  $T_g$  for PETG composites. The interfacial interaction between graphene and PETG plays a crucial role in enhancing the thermal stability of the composite material. Graphene, with its high thermal conductivity and stability, serves as a reinforcing agent that disperses uniformly in the PETG matrix, improving its thermal properties. The interfacial interaction between graphene and PETG enhances the degree of crystallinity and



thermal stability of PETG. It also restricts the mobility of PETG molecules and reduces the degree of thermal degradation by preventing the release of volatile products. This leads to improved thermal stability of the composite material, making it suitable for various high-temperature applications.

This study provides important new information about the initial thermal characteristics of PETG composites reinforced with graphene. Despite the lack of a thorough analysis of their mechanical properties, these discoveries set the groundwork for possible uses of these polymer composites in the production of airplane interior components and minor automobile parts. To determine these composites' appropriateness in practical situations, future studies will concentrate on thorough analyses of their mechanical, electromagnetic, and rheological behavior.

### ACKNOWLEDGMENTS

The financial support of the NIT Trichy through the Seed Grant (NITT/R&C/SEED GRANT/2021-22/PROJ.NO.49) is sincerely acknowledged by the authors, Surjeet Singh Bedi and Vasu Mallesha. The financial support of the Department of Science and Technology (DST) through the Scheme for Young Scientists and Technologists (SP/YO/2021/1652) is sincerely acknowledged by the author, Vinyas Mahesh.

### CONFLICT OF INTEREST STATEMENT

None.

### DATA AVAILABILITY STATEMENT

The raw/processed data required to reproduce these findings cannot be shared at this time as the data also forms part of an ongoing study.

### ORCID

Vasu Mallesha  <https://orcid.org/0000-0001-7477-2415>

Vinyas Mahesh  <https://orcid.org/0000-0001-8394-1321>

Vishwas Mahesh  <https://orcid.org/0000-0002-1315-9462>

### REFERENCES

- Bao YZ, Cong LF, Huang ZM, Weng ZX. Preparation and proton conductivity of poly (vinylidene fluoride)/layered double hydroxide nanocomposite gel electrolytes. *J Mater Sci.* 2008;43:390-394.
- Liu N, Luo F, Wu H, Liu Y, Zhang C, Chen J. One-step ionic-liquid-assisted electrochemical synthesis of ionic-liquid-functionalized graphene sheets directly from graphite. *Adv Funct Mater.* 2008;18(10):1518-1525.
- El Moumen A, Tarfaoui M, Lafdi K. Additive manufacturing of polymer composites: processing and modeling approaches. *Compos Part B Eng.* 2019;171:166-182.
- Parandoush P, Lin D. A review on additive manufacturing of polymer-fiber composites. *Compos Struct.* 2017;182:36-53.
- Dreyer DR, Park S, Bielawski CW, Ruoff RS. The chemistry of graphene oxide. *Chem Soc Rev.* 2010;39(1):228-240.
- Wang G, Yang J, Park J, et al. Facile synthesis and characterization of graphene nanosheets. *J Phys Chem C.* 2008;112:8192-8195.
- Wang G, Shen X, Wang B, Yao J, Park J. Synthesis and characterization of hydrophilic and organophilic graphene nanosheets. *Carbon.* 2009;47(5):1359-1364.
- Li X, Wang X, Zhang L, Lee S, Dai H. Chemically derived, Ultrasmooth graphene nanoribbon semiconductors. *Science.* 2008;319:1229-1232.
- Allen MJ, Tung VC, Kaner RB. Honeycomb carbon: a review of graphene. *Chem Rev.* 2010;110:132-145.
- Stankovich S, Dikin DA, Dommett GH, et al. Graphene-based composite materials. *Nature.* 2006;442(7100):282-286.
- Paran SMR, Naderi G, Ghoreishy MHR, Heydari A. Enhancement of mechanical, thermal and morphological properties of compatibilized graphene reinforced dynamically vulcanized thermoplastic elastomer vulcanizates based on polyethylene and reclaimed rubber. *Compos Sci Technol.* 2018;161:57-65.
- Bera M, Maji PK. Effect of structural disparity of graphene-based materials on thermo-mechanical and surface properties of thermoplastic polyurethane nanocomposites. *Polymer.* 2017;119:118-133.
- Pandey N, Tewari C, Dhali S, et al. Effect of graphene oxide on the mechanical and thermal properties of graphene oxide/hytrex nanocomposites. *J Thermoplast Compos Mater.* 2021;34(1):55-67.
- Liu Q, Zhou X, Fan X, Zhu C, Yao X, Liu Z. Mechanical and thermal properties of epoxy resin nanocomposites reinforced with graphene oxide. *Polym-Plast Technol Eng.* 2012;51(3):251-256.
- Liao KH, Qian Y, Macosko CW. Ultralow percolation graphene/polyurethane acrylate nanocomposites. *Polymer.* 2012;53(17):3756-3761.
- Wang B, Li N, Cheng S, et al. Thermal conductivity and mechanical properties enhancement of CF/PPBESK thermoplastic composites by introducing graphene. *Polym Compos.* 2022;43(5):2736-2745.
- Zandiatashbar A, Picu RC, Koratkar N. Mechanical behavior of epoxy-graphene platelets nanocomposites. *J Eng Mater Technol.* 2012;134(3):031011.
- Yang SY, Lin WN, Huang YL, et al. Synergetic effects of graphene platelets and carbon nanotubes on the mechanical and thermal properties of epoxy composites. *Carbon.* 2011;49(3):793-803.
- Ahmadi-Moghadam B, Taheri F. Effect of processing parameters on the structure and multi-functional performance of epoxy/GNP-nanocomposites. *J Mater Sci.* 2014;49:6180-6190.
- Li W, Dichiaro A, Bai J. Carbon nanotube-graphene nanoplatelet hybrids as high-performance multifunctional reinforcements in epoxy composites. *Compos Sci Technol.* 2013;74:221-227.
- Zhu Y, Murali S, Cai W, et al. Graphene and graphene oxide: synthesis, properties, and applications. *Adv Mater.* 2010;22(35):3906-3924.
- Sethuram D, Koppad PG, Shetty H, Alipour M, Kord S. Characterization of graphene reinforced Al-Sn nanocomposite produced by mechanical alloying and vacuum hot pressing. *Mater Today Proc.* 2018;5(11):24505-24514.
- Zhou M, Bi H, Lin T, Lü X, Huang F, Lin J. Directional architecture of graphene/ceramic composites with improved

- thermal conduction for thermal applications. *J Mater Chem A*. 2014;2(7):2187-2193.
24. Yang H, Shan C, Li F, Zhang Q, Han D, Niu L. Convenient preparation of tunably loaded chemically converted graphene oxide/epoxy resin nanocomposites from graphene oxide sheets through two-phase extraction. *J Mater Chem*. 2009;19(46):8856-8860.
  25. Tambrallimath V, Keshavamurthy R, Saravanbavan D, Kumar GP, Kumar MH. *Synthesis and characterization of graphene filled PC-ABS filament for FDM applications*. In AIP Conference Proceedings (Vol. 2057, No. 1, p. 020039). AIP Publishing LLC; 2019.
  26. Relinque JJ, Romero-Ocaña I, Navas-Martos FJ, Delgado FJ, Domínguez M, Molina SI. Synthesis and characterization of enhanced conductivity acrylonitrile-butadiene-styrene based composites suitable for fused filament fabrication. *Polym Compos*. 2022;43(9):6611-6623.
  27. Patra NR, Negi YS. Thermal, structural, and rheological modifications in recycled polyethylene terephthalate for a sustainable alternative source for additive manufacturing. *Polym Eng Sci*. 2022;62(8):2486-2497.
  28. Mahesh V, Joseph AS, Mahesh V, Harursampath D. Thermal characterization of organically modified montmorillonite and short carbon fibers reinforced glycol-modified polyethylene terephthalate nanocomposite filaments. *Polym Compos*. 2021; 42(9):4478-4496.
  29. Sahoo NG, Cheng HKF, Cai J, et al. Improvement of mechanical and thermal properties of carbon nanotube composites through nanotube functionalization and processing methods. *Mater Chem Phys*. 2009;117(1):313-320.
  30. Billah KMM, Lorenzana FA, Martinez NL, Wicker RB, Espalin D. Thermomechanical characterization of short carbon fiber and short glass fiber-reinforced ABS used in large format additive manufacturing. *Addit Manuf*. 2020;35:101299.
  31. Ramanathan T, Abdala AA, Stankovich S, et al. Functionalized graphene sheets for polymer nanocomposites. *Nat Nanotechnol*. 2008;3(6):327-331.
  32. El Achaby M, Arrakhiz FE, Vaudreuil S, el Kacem Qaiss A, Bousmina M, Fassi-Fehri O. Mechanical, thermal, and rheological properties of graphene-based polypropylene nanocomposites prepared by melt mixing. *Polym Compos*. 2012;33(5):733-744.

**How to cite this article:** Bedi SS, Mallesha V, Mahesh V, et al. Thermal characterization of 3D printable multifunctional graphene-reinforced polyethylene terephthalate glycol (PETG) composite filaments enabled for smart structural applications. *Polym Eng Sci*. 2023;1-16. doi:[10.1002/polb.26409](https://doi.org/10.1002/polb.26409)